CHIN.PHYS.LETT. Vol. 19, No. 5 (2002) 666

Modified Two-Scale Model for Low-Grazing-Angle Scattering from Two-Dimensional Sea Surface *

ZHANG Yan-Dong (张延冬) , WU Zhen-Sen(吴振森)
School of Sciences, Xidian University, Xi'an 710071

(Received 19 November 2001)

A hybrid model for describing a fully developed two-dimensional sea surface is presented, which incorporates the sea spectrum into a fractal model, and an improved two-scale model is applied to calculate the scattering coefficient. In this model the slope distribution of the large-scale surface is obtained with a numerical method instead of being assumed, and the projecting and ray tracing methods are applied to obtain the shadow function for arbitrary incident and scattering angles. Moreover the effect of curvature of the large-scale undulating surface on the scattered wave is taken into account. Hence the precision of the results is greatly increased at low-grazing angles. Finally the amplitude and fractal characteristics of the scattered wave are analysed, which are of great significance for distinguishing and detecting targets on the sea.

PACS: 41. 20. − q, 42. 25. Bs, 42. 25. Dd

Since the invention of radar, the study of electromagnetic scattering from rough sea surfaces has been widely used in remote sensing, distinguishing and detecting targets, etc. The model of a rough sea surface is often necessary to study electromagnetic scattering. The sea surface is a complex but not totally random rough surface. So far there have been many kinds of methods on modelling a rough sea surface and they might be divided into two categories: statistical[1] and fractal.[2−4] The statistical methods can be applied to model a rough sea surface with an arbitrary form of spectrum, but this is totally random and cannot agree well with the real sea surface. In general, the sea surface is made up of quasi-periodic waves and disordered foam, ripple and spray superposed on the large-scale one, i.e. two average sizes of roughness, therefore it is difficult to describe it with conventional Euclidean geometry. With the advent of fractal geometry, this has been used to model sea surfaces since it can represent the characteristics of sea surfaces; namely, the mix of long-range order and short-range disorder. However, the spectrum of the fractal model only satisfies the inverse power law, so it is insufficient to describe the rough sea surface only with the fractal model. Here we shall incorporate a sea spectrum that agrees well with the experimental data into the fractal model to represent a fully developed sea surface. In this model, quasi-periodic functions are used as the elementary function for the sea surface while the sea spectrum serves as the weight function.[5,6] Taking the variation of the sea surface with time into account we can model the two-dimensional rough sea surface by

$$f(x,y) = \sigma C \sum_{i=1}^{i\max} \sum_{j=1}^{j\max} S(k_{xi}, k_{yj}) \sum_{n=0}^{N-1} b^{(D-3)n} \cdot \sin\left[k_0 b^n (k_{xi} x \cos\theta_n + k_{yj} y \sin\theta_n) + \sqrt{g k_0} b^{n/2} t + \varphi_n\right], \quad (1)$$

where all the parameters except $S(k_x, k_y)$ are the same as those in the band limited Weierstrass fractal function. The semi-empirical sea spectrum $S(k_x, k_y)$ developed by Fung[7] is shown as follows

$$S(k,\phi) = S(k)\left[a_0 + a_1\left(1 - \mathrm{e}^{-bk^2}\right)\cos 2\phi\right], \quad (2)$$

where $S(k)$ is the one-dimensional sea spectrum, a_0, a_1 and b are the constants depending on wind speed, and ϕ is the included angle between the relevant direction and the direction of wind. Hence the difference between downwind and crosswind is taken into account in this spectrum. Many theories for the prediction of electromagnetic scattering from the sea surface have been developed recently. For the sea surface it contains many spatial scales, ranging from long gravity type sea waves that can have wavelengths of hundreds of metres to short capillary type sea waves that can have wavelengths in the millimetre range. For this kind of rough surface it is convenient to solve its electromagnetic scattering with the two-scale model.[8,9] The two-scale model states that scattering from such a surface can be calculated by dividing the surface spectrum into a "long" wavelength portion, for which the Kirchhoff approximation (KA) holds, and a "short" wavelength portion, for which the small perturbation method (SPM) can be applied. However, SPM predictions are averaged over the slope distribution of the long waves to model the long wave tilting effect on the short wave portion of the spectrum. When the incident angle or scattering angle increases in the Kirchhoff approximation, especially for a low grazing angle, the difference between results by numeric calculation and experimental results increases substantially, hence further modification is needed. In this Letter, the conventional two-scale method with curvature modification is proposed, and on the basis of the sea surface generated by the hybrid model the slope and curvature radius at any point on the large-scale roughness are obtained with the difference method. Therefore we can avoid assuming the probability density function of the slope and curvature. In addition, for large incident angle the shadowing effect should be taken into account. In the past some empirical formulae

*Supported by the National Natural Science Foundation of China under Grant No 60081002.
©2002 Chinese Physical Society and IOP Publishing Ltd

were adopted to describe the shadowing effect,[10,11] but they hold only for some cases. For a large incident angle some facets of the sea surface cannot be illuminated by the incident wave due to the shadowing of others, and similarly for a large scattering angle the scattered wave by some facets cannot be received. In this Letter the projecting and ray tracing methods are introduced to calculate the shadow function for arbitrary incident and scattering angles, which are called the incident shadowing and scattering shadowing, respectively. Taking the incident shadowing for example, each facet of the rough surface is projected onto a plane $\hat{x}'\hat{y}'$ called the projection plane that is perpendicular to incident direction (θ_i, φ_i). The projection plane is defined as follows

$$\hat{z}' = -\hat{k}_i = -\sin\theta_i\cos\varphi_i\hat{x} - \sin\theta_i\sin\varphi_i\hat{y} + \cos\theta_i\hat{z}$$

$$\begin{aligned}\hat{y}' &= \frac{\hat{z}'\times\hat{x}}{|\hat{z}'\times\hat{x}|} = \frac{\cos\theta_i\hat{y} + \sin\theta_i\sin\varphi_i\hat{z}}{\sqrt{\cos^2\theta_i + \sin^2\theta_i\sin^2\varphi_i}}\\ \hat{x}' &= \hat{y}'\times\hat{z}' = [\left(\cos^2\theta_i + \sin^2\theta_i\sin^2\varphi_i\right)\hat{x}\\ &\quad - \sin^2\theta_i\sin\varphi_i\cos\varphi_i\hat{y} + \sin\theta_i\cos\theta_i\cos\varphi_i\hat{z}]\\ &\quad \cdot \left(\cos^2\theta_i + \sin^2\theta_i\sin^2\varphi_i\right)^{-1/2}. \end{aligned} \tag{3}$$

For each facet we first determine whether its projection has areas in common with the others. If so, we then decide whether the facet is shadowed by another according to the position of the two facets relative to the incident direction. The total shadowed area of each facet can be obtained according to this rule, then summing and dividing by the total area of all facets will lead to the incident shadowing function. Similarly the scattering shadowing function can be obtained. The total shadowing function is the product of incident self-shadowing, incident shadowing, scattering self-shadowing and scattering shadowing function.

$$S(\theta_i, \theta_s) = S_1(\theta_i)\cdot S_2(\theta_i)\cdot S_3(\theta_s)\cdot S_4(\theta_s). \tag{4}$$

In particular, the smoothness of the large-scale surface component is a very crucial requirement for the KA mentioned above, because the KA actually neglects the diffraction of incident field on an undulating surface. This neglect imposes a strong limitation on surface curvatures[12]

$$k_0 R\sin^3\theta_g \gg 1. \tag{5}$$

where $k_0 = 2\pi/\lambda$ is the radiation wavenumber, R is the main curvature radius of a surface large-scale component in the plane of incidence, and θ_g is the grazing angle with respect to the mean surface plane. For typical sea roughness spectra this limitation leads to a failure of the KA for $\theta_g < 20^\circ$. Therefore, at these grazing angles the facets composing a large-scale component of the rough sea surface must be considered as curved elements rather than flat ones.

A two-dimensional sea surface has more roughness in the downwind direction than that in the crosswind direction, therefore it is feasible only to consider the effect of the curvature of large-scale roughness in the downwind direction on the scattered wave. Let downwind orientate to the x-axis, then the formula in the conventional two-scale method can be modified as

$$\begin{aligned}\sigma_{HH}(\theta) = &\int_{-\infty}^{\infty} \mathrm{d}R_x \int_{-\mathrm{ctg}\theta}^{\infty}\int_{-\infty}^{\infty} \left(\hat{h}\cdot\hat{h}'\right)^4\\ &\cdot \sigma_{hh}(\theta')\, c_{HH}\left(\theta', \frac{\omega}{c}R_x\right)(1 + z_x\mathrm{tg}\theta)\\ &\cdot P(z_x, z_y, R_x)\,\mathrm{d}z_x\mathrm{d}z_y, \end{aligned} \tag{6}$$

$$\begin{aligned}\sigma_{VV}(\theta) = &\int_{-\infty}^{\infty} \mathrm{d}R_x \int_{-\mathrm{ctg}\theta}^{\infty}\int_{-\infty}^{\infty} (\hat{v}\cdot\hat{v}')^4\\ &\cdot \sigma_{vv}(\theta')\; c_{VV}\left(\theta', \frac{\omega}{c}R_x\right)(1 + z_x\mathrm{tg}\theta)\\ &\cdot P(z_x, z_y, R_x)\,\mathrm{d}z_x\mathrm{d}z_y, \end{aligned} \tag{7}$$

where $c_{VV}(\theta', \omega R_x/c)$ and $c_{HH}(\theta', \omega R_x/c)$ are the modified factors depending on the x-components of curvature radius. In Eqs. (6) and (7) the probability density functions of the slope and curvature radius of the large-scale roughness are unknown. In the past they were assumed to satisfy Gauss or Weibull distributions and this assumption remains to be confirmed. Here the large-scale slope along the x- and y-directions can be calculated with the centred difference method on the basis of the generated large-scale surface. Then the x-components of curvature radius can be obtained. Supposing that the distribution of slope and curvature is independent, we have $P(z_x, z_y, R_x) = P(z_x, z_y)\cdot P(R_x)$.[13] Upon substituting summation for the integration in Eqs. (6) and (7), and with regard to the shadowing effect we obtain

$$\begin{aligned}\sigma_{HH}(\theta) = &\frac{1}{N_x^2}\frac{1}{N_y}\sum_{i=1}^{N_x}\sum_{j=i}^{N_y}\sum_{k=1}^{N_x}\left(\hat{h}\cdot\hat{h}'\right)^4\\ &\cdot \sigma_{hh}(\theta')\, c_{HH}\left[\theta', \frac{\omega}{c}R_x(x_k, y_j)\right]\\ &\cdot [1 + z_x(x_i, y_j)\,\mathrm{tg}\theta]\cdot S(\theta_i, \theta_s), \end{aligned} \tag{8}$$

$$\begin{aligned}\sigma_{VV}(\theta) = &\frac{1}{N_x^2}\frac{1}{N_y}\sum_{i=1}^{N_x}\sum_{j=i}^{N_y}\sum_{k=1}^{N_x}(\hat{v}\cdot\hat{v}')^4\\ &\cdot \sigma_{vv}(\theta')\, c_{VV}\left[\theta', \frac{\omega}{c}R_x(x_k, y_j)\right]\\ &\cdot [1 + z_x(x_i, y_j)\,\mathrm{tg}\theta]\cdot S(\theta_i, \theta_s), \end{aligned} \tag{9}$$

where N_x and N_y are the total points when the sea surface is modelled.

The two-dimensional sea surface is generated using the hybrid model, 500 m in length and width. The frequency of the incident wave is chosen to be $f = 13.9$ GHz. The slope distributions of generated two-dimensional rough sea surface at different wind speeds are displayed in Figs. 1 and 2. Since the wind direction is chosen to be along the x-axis, the sea surface has more roughness along the x-direction than along the y-direction. Hence this leads to the narrower width and higher peak of the curves in Fig. 1 compared to the corresponding ones in Fig. 2, which justifies the approximation in our calculation that the curvature effect along the y-direction is neglected.

The dependence of the backscattering coefficient

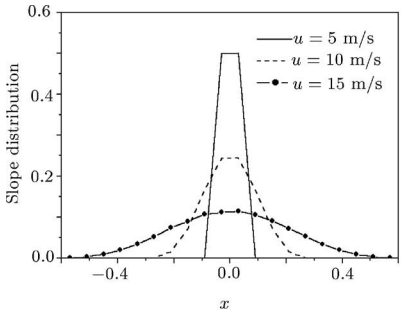

Fig. 1. Slope distribution along the x-direction.

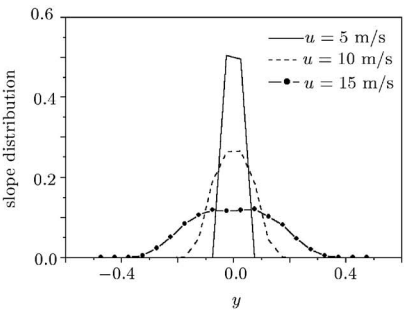

Fig. 2. Slope distribution along the y-direction.

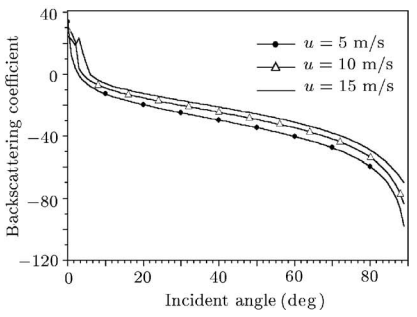

Fig. 3. Dependence of backscattering coefficient for different wind speeds.

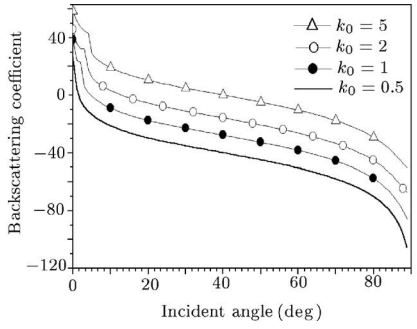

Fig. 4. Dependence of backscattering coefficient for different fundamental spatial wavenumber k_0.

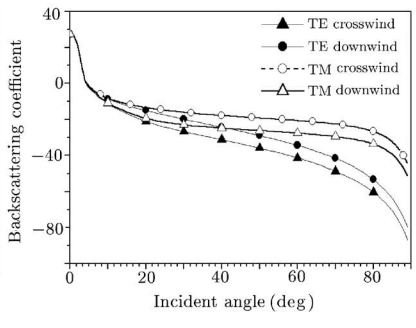

Fig. 5. Comparison of downwind and crosswind.

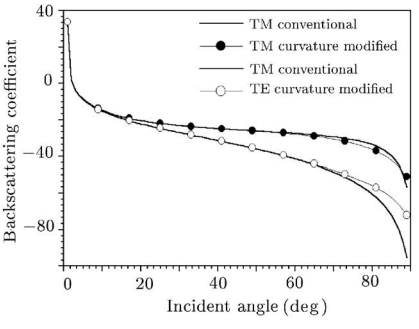

Fig. 6. Effect of curvature modification.

as well as the effect of the curvature modification on the incident angle, wind speed and wind direction is discussed, and the amplitude characteristic and fractal characteristic of scattered wave are also analysed, which are useful in engineering.

The variation of the backscattering coefficient with incident angle at different wind speeds is displayed in Fig. 3. As can be seen, the backscattering coefficient declines more slowly as the wind speed increases since higher wind speed leads to a rougher surface, hence the coherent component declines while the diffuse component increases. Figure 4 shows the effect of the fundamental spatial wavenumber on the backscattering coefficient. Since the fundamental spatial wavenumber affects the slope variances of the generated sea surface, its effect on the backscattering coefficient is similar to that of wind speed. The effect of downwind and crosswind on the backscattering coefficient for different polarizations is demonstrated in Fig. 5. For the incident wave the sea surface has more roughness in the downwind direction than the crosswind direction, hence the downwind backscattering coefficient will decline more slowly as the incident angle increases.

Comparing the conventional and the curvature-modified two-scale methods in Fig. 6, we can see that when the curvature effect is taken into account for low grazing angle, the backscattering coefficient will decline more slowly as the incident angle increases in both horizontal and vertical polarizations, which is due to the occupation of diffraction. To test its validity, we carry out a comparison of the polarization radio σ_{HH}/σ_{VV} by the conventional and the curvature-modified two-scale methods with experimental data.[14] As can be seen in Fig. 7, taking the curvature effect into account leads to better agreement between theoretical and experimental results. In addition, the variation of the backscattering coefficient with wind speed at different incident angles in horizontal polarization is obtained and compared with experimental data,[15] as demonstrated in Figs. 8 and 9, where dots represent the experimental data and solid lines represent the theoretical results. Figures 8 and 9 show the behaviour of the downwind and crosswind, respectively. From these we can find that, for fairly low wind speed, the theoretical results are in good agreement with the experimental data. However, the error between them both begins to arise when the wind speed increases. This may be interpreted as follows. The two-scale model can only be applied to calculate surface scattering, however the foam arises when the wind speed increases. They also dedicate to the scattered wave we call the volume scattering, hence the theoretical results are slightly smaller than the experimental data.

To analyse the amplitude distribution of scattered waves, we generate a sequence of the backscattering coefficient and calculate its fractal dimension using the box-counting method. The dependence of the fractal dimension of the scattered wave on incident angle and fractal dimension of the sea surface is demonstrated

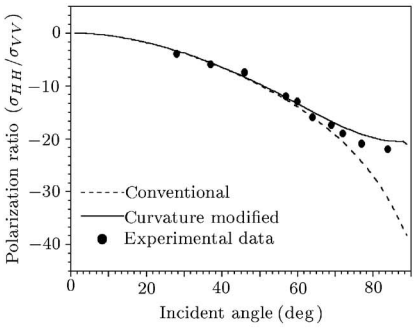

Fig. 7. Effect of curvature modification ($v = 6$ m/s).

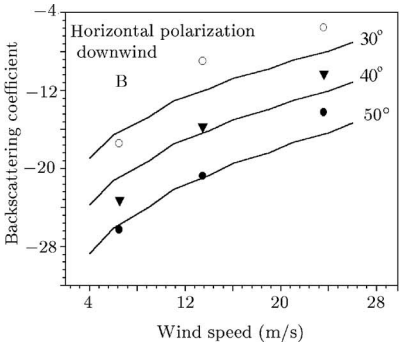

Fig. 8. Variation of backscattering coefficient with wind speed.

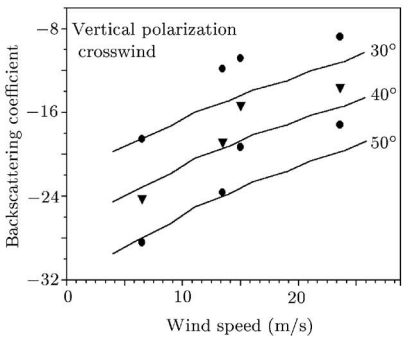

Fig. 9. Variation of backscattering coefficient with wind speed.

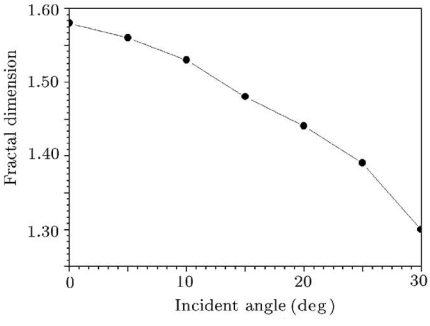

Fig. 10. Variation of fractal dimension of scattered wave with incident angle.

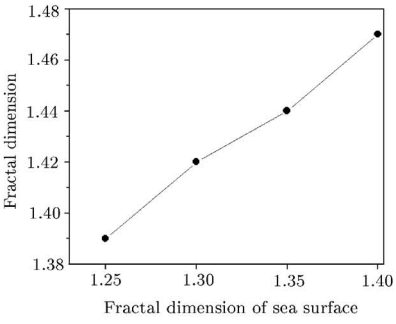

Fig. 11. Variation of fractal dimension of scattered wave with that of sea surface.

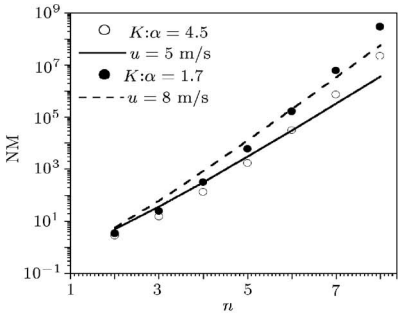

Fig. 12. Comparison of amplitude distribution of scattered wave with K-distribution.

in Figs. 10 and 11. It can be seen from Fig. 10 that the fractal dimension of the scattered wave increases as that of the sea surface increases, which can be used to detect targets on the sea since targets and sea surface have different fractal dimensions. From Fig. 11 we can conclude that the fractal dimension of the scattered wave declines with the increase of incident angle, which may be interpreted by the Rayleigh criterion. To obtain the amplitude distribution of the scattering wave, we carry out a comparison of normalized n-order moments between the backscattering coefficient and the K-distribution, as shown in Fig. 12, from which it can be concluded that the amplitude distribution of scattering wave is in good agreement with the K-distribution.

In conclusion, a hybrid model for describing the fully developed two-dimensional sea surface is presented, which incorporates the sea spectrum into the fractal model. It can not only embody the characteristic of long-range order and short-range disorder of the sea surface but also imposes no limitation on the form of the sea spectrum. The two-scale method is applied to calculate the scattering coefficient, and the value of the large-scale slope is obtained with the centred difference method. Therefore we can avoid assuming the probability density function of the slope. Then the projecting and ray tracing methods are applied to obtain the shadow function for arbitrary incident and scattering angles, and the effect of curvature of the large-scale undulating surface is taken into account. Hence the two-scale model can remain accurate for low grazing angles. Finally the amplitude and fractal characteristics of the scattered wave are analysed. It can be concluded from the results that the amplitude of the scattered wave satisfies the K-distribution, the scattered wave is also fractal and its fractal dimension is proportional to that of the rough sea surface and is proportional inversely to the incidence angle, which are of great significance for distinguishing and detecting targets on the sea.

References

[1] Thorsos E I 1988 *J. Acoust. Soc. Am.* **83** 78
[2] West B J 1990 *J. Opt. Soc. Am.* A **7** 1074
[3] Jaggard D L and Sun X G 1990 *J. Opt. Soc. Am.* A **7** 1131
[4] Guo L X and Wu Z S 2001 *Chin. Phys. Lett.* **18** 42
[5] Guo L X and Wu Z S 2000 *J. Phys.* **49** 1064
[6] Chen J, Lo T K Y, Leung H 1996 *IEEE Trans. Geosci. Remote Sensing* **34** 966
[7] Fung A K 1982 *IEEE J. Oceanic Eng.* **7** 166
[8] Ulaby F T, Moore R K and Fung A K 1982 *Microwave Remote Sensing* (Canada: Addison-Wesley)
[9] Johnson J T, Shin R T and Kong J A 1998 *IEEE Trans. Geosci. Remote Sensing* **36** 72
[10] Wagner R J 1967 *J. Acoust. Soc. Am.* **41** 138
[11] Hsieh C Y et al 1997 *IEEE Trans. Geosci. Remote Sensing* **35** 901
[12] Voronovich A G 1996 *Radio Sci.* **31** 1519
[13] Voronovich A G 1998 *Waves Random Media* **8** 41
[14] Lee P H Y and Barter J D et al 1995 *J. Geophys. Res.* **100** 591
[15] Jones W L et al 1977 *IEEE Trans. Antennas Propag.* **25** 84